International Journal of Solids and Structures 100–101 (2016) 332–340

Contents lists available at ScienceDirect

International Journal of Solids and Structures

journal homepage: www.elsevier.com/locate/ijsolstr

Dynamic crack branching and curving in brittle polymers

Jooeun Lee, Jung-Wuk Hong*

Department of Civil and Environmental Engineering, Korea Advanced Institute of Science and Technology, Daejeon 34141, South Korea

ARTICLE INFO

Article history:
Received 23 November 2015
Revised 5 August 2016
Available online 17 September 2016

Keywords:
Crack branching
Crack curving
Brittle polymers
Dynamic fracture
Peridynamics

ABSTRACT

This paper presents peridynamics simulation on crack branching and curving in a pre-existing center-notched brittle polymer. Fracturing patterns in brittle polymer under a biaxial tensile loading condition are compared with experimental observations for validation. Then, several numerical examples are conducted in order to investigate crack initiation and propagation of the pre-existing center notch under the effect of different loading ratios. Further to this, the crack development sequences of branching and curving are in detail discussed, and their underlying causes are identified through various perspectives including crack curving and branching angles, elastic strain energy, and branching damage patterns. The numerical results reasonably reflect the physical observations. This paper both complements the test results and provides insightful information for the prediction of crack branching and curving in brittle polymers.

1. Introduction

Brittle materials are at greater risk of being exposed to abrupt fractures caused by the nucleation and development of numerous micro-cracks. Such micro-voids and micro-defects can foster crack initiations, thereby degrading the mechanical performance of brittle materials. This damage can be also affected by external environments such as loading configuration, stress levels, and initial cracks. Hence, accurate measurement of the initiation and propagation of defects has been an issue of great interest among researchers in the last decades. However, numerical predictions and experimental determination of the preexisting crack damage (or defects and voids) have remained as one of the challenges in its relevant fields as well as fracture mechanics. Moreover, no comprehensive data have been reported on specific fracturing mechanisms such as crack branching and curving (Ha and Bobaru, 2010).

As for experimental study of crack branching and curving, Hawong et al. (1987) performed experiments on crack branching and curving in Homalite-100 under biaxial loading conditions. They observed effects of biaxial stress ratios of horizontal loading to vertical loading (0.0 to 3.7) on an initially horizontal crack. For a loading ratio of 0.33, the crack propagated horizontally and then bifurcated at some distance from the crack tip, resulting in two branches. The damage patterns were symmetrical to some degree, but damage patterns in the cases with other than 0.33 were unstable and unsymmetrical partially due to the fact that keeping loadings constant is difficult in a real physical experiment. Shukla and Anand (1986) investigated crack propagation and branching under biaxial loading experimentally. The researchers demonstrated that tensile stress parallel to the crack increases crack curving noticeably, and tension–tensing loading yields branching angles that are equal to or larger than 73°. Many researchers including Cotterell (1966, 1965), Cotterell and Rice (1980), Leevers and Radon (1982), and Leevers et al. (1977) reported that the tensile stress causes higher stress intensity factors compared with its compression counterpart and that tensile stress produces branching at some level. Fineberg et al. (1992, 1991) also extensively studied on crack branching and curving. Murphy et al. (2006) conducted a physical test on crack branching patterns of small poly(methyl methacrylate) single-edge notched tensile specimens. They observed that macroscopic branching generally occurs at an angle of 25°.

Yu et al. (2006) conducted finite element simulations to predict crack patterns at different strain rates in poly(methyl methacrylate) and Homalite-100. At lower strain rates, the observed single crack was smooth and straight. However, at a higher strain rate, the crack propagates for a shorter distance and then small side branches emanate from the main crack. Yang et al. (2012) used the dynamic version of RFPA2D to predict crack propagation in pre-existing center notched slabs under dynamic biaxial tensile loading. They investigated the effect of different stress configurations, different stress levels, heterogeneity, and the crack tip angle for rock materials. When the biaxial loading ratios increased from 1.16 to 3.05, the crack curvature also increased. In addition, the crack propagated approximately perpendicular to the exerting direction of the larger stress level. The crack propagation speed oscillates

* Corresponding author.
E-mail addresses: j.hong@kaist.ac.kr, jwhong@alum.mit.edu (J.-W. Hong).

http://dx.doi.org/10.1016/j.ijsolstr.2016.09.002
0020-7683/

gently around a certain value during crack propagation. However, the crack angle used in the test models was set to 20° rather than the horizontal crack in physical experiments (Hawong et al., 1987) in order to consider asymmetrical crack branching patterns under the effect of instability in the physical experiments. Similarly, Rafiee et al. (2003) set the initial crack at a slight slant of 5° to cause a geometric imperfection, which leads to asymmetric damage patterns. Zhang et al. (2012) considered the effect of biaxial loading ratio and heterogeneity on the evolution of crack branching using RFPA2D-Dynamic Code. Under uniaxial loading conditions, they observed that the branching angle in homogeneous materials is approximately 23.7° as shown in experimental results (Murphy et al., 2006). As the ratio of horizontal to vertical loading increases, the macroscopic branching angle was observed to increase with multiple emerging microscopic cracks.

Silling (2000) developed the peridynamic formulation in which discontinuities such as voids and cracks are modeled without introducing other formulations or techniques including dissimilar mathematical methods or remeshing. Therefore, this methodology has been used by many researchers since then. Bobaru and Hu (2012) used peridynamics to investigate the influence of horizon size on crack branching in the brittle polymer, Homalite-100, and proposed an appropriate horizon size. They also reported that the branching angle is independent of the horizon size if no interaction occurs between the crack and stress waves, and the waves control the crack path and curving. Ha and Bobaru (2010) investigated dynamic crack propagation and crack branching in soda-lime glass and Duran 50 glass. The effects of different (constant and conical) micromoduli were studied, and a convergence study for dynamic crack branching was performed. Agwai et al. (2008) investigated crack propagation in a glass plate under different loading rates. They concluded that crack branching behaviors depend on the loading conditions. Kilic and Madenci (2009) presented the effects of temperature gradients on crack growth in a glass plate with a single and multiple initial cracks. Liu and Hong (2012c) simulated crack propagation in concrete that was subjected to biaxial tension and shear with a coupling method. Lee et al. (2016a, b, c) investigated the crack development sequences and identified their underlying causes using parallelized peridynamics coupled with finite element method. Numerical results obtained through peridynamics show a very good agreement with physical observations.

In this paper, we summarize the basic theory of peridynamic formulation. Then, we explain the numerical model, including the specimen geometry, traction boundary condition, and dynamic loading. Then, numerical results obtained through peridynamic simulation are compared with experimental results for validation and verification of the simulation. The crack development sequences of crack branching and curving in brittle polymer are in detail discussed, and their underlying causes are investigated through damage maps, elastic strain energy maps, crack tip displacements, crack tip maximum strain energies, and crack tip propagation speeds.

2. Summary of peridynamics

2.1. Overview of peridynamic formulation

Linear momentum in classical continuum mechanics is given by:

$$\rho\,\ddot{\mathbf{u}}(\mathbf{x}) = \nabla\cdot\boldsymbol{\sigma} + \mathbf{b} \tag{1}$$

where ρ denotes density, $\ddot{\mathbf{u}}$ is the acceleration vector, $\boldsymbol{\sigma}$ is the stress matrix, and $\mathbf{b}$ is the body force vector. Here, the canonical divergence of the stress tensor is not unique. Therefore, to calculate discontinuity, the canonical divergence is reformulated by an integral operator, which sums a number of forces within a finite distance (Silling, 2000; Agwai et al., 2008; Silling and Lehoucq, 2010), and the momentum equation is rewritten as:

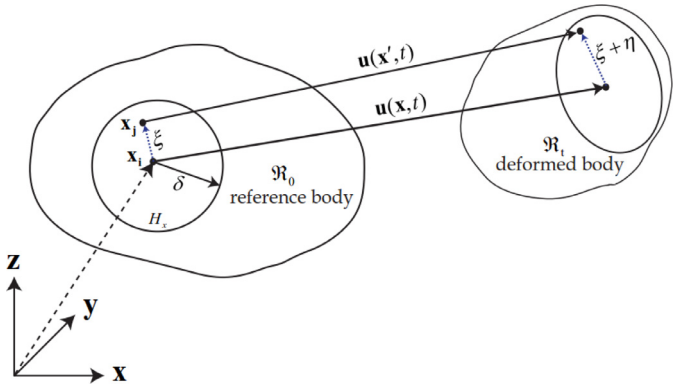

Fig. 1. Schematic of peridynamic bond deformation.

$$\rho\,\ddot{\mathbf{u}}(\mathbf{x},t) = \int_{R_i}\mathbf{f}(\boldsymbol{\eta},\boldsymbol{\xi})\,dV_j + \mathbf{b}(\mathbf{x_i}+t) \tag{2}$$

where ρ represents the mass density, $\mathbf{u}$ is the displacement vector field, $\mathbf{f}$ is the interacting force vector, R_i is a spherical neighborhood of particles interacting with the particle i, dV_j denotes an infinitesimal volume linked to particle j, and $\mathbf{b}$ is a prescribed body force density field. In the peridynamic formulation, the horizon δ governs the interacting spatial range between particles i and j. Hence, if the distance between two particles is larger than the horizon, the interacting force between a pair of particles is non-existent. The interacting force vector $\mathbf{f}(\boldsymbol{\eta},\boldsymbol{\xi})$ is written as:

$$\mathbf{f}(\boldsymbol{\eta},\boldsymbol{\xi}) = F(\boldsymbol{\eta},\boldsymbol{\xi})\,\frac{\boldsymbol{\eta}+\boldsymbol{\xi}}{\|\boldsymbol{\eta}+\boldsymbol{\xi}\|} \tag{3}$$

where $F(\boldsymbol{\eta},\boldsymbol{\xi})$ denotes the scalar-valued pairwise force function, and $\frac{\boldsymbol{\eta}+\boldsymbol{\xi}}{\|\boldsymbol{\eta}+\boldsymbol{\xi}\|}$ denotes the direction of the interaction force between particles i and j, as shown in Fig. 1. Accordingly, the pairwise force scalar $F(\boldsymbol{\eta},\boldsymbol{\xi})$ is discretized as:

$$F(\boldsymbol{\eta},\boldsymbol{\xi}) = \left(\mu(t,\boldsymbol{\xi})\cdot c\cdot s(\boldsymbol{\eta},\boldsymbol{\xi})\right) \tag{4}$$

where $\mu(t,\boldsymbol{\xi})$ is a history-dependent scalar-valued function, c is the micromodulus, $s(\boldsymbol{\eta},\boldsymbol{\xi})$ is the bond stretch between particles i and j, and s_0 is the critical bond stretch for bond failure. The critical bond stretch s_0 for brittle materials in the peridynamic formulation is calculated by the breakage of all bonds per unit fracture area from the energy release rate G_f (Silling and Askari, 2005), and k is bulk modulus.

$$s_0 = \sqrt{\frac{5G_f}{9k\delta}} \tag{5}$$

For numerical analysis, Eq. (2) is implemented with two discretization processes: spatial discretization using a 'sum' instead of integration, and temporal discretization using the speed-Verlet scheme (Ercolessi, 1997). The equation of motion in the peridynamic formulation after the discretization is described as:

$$\rho\ddot{\mathbf{u}}_i^{(t)} = \sum_{j=1}^{j=N_{R_i}}\mathbf{f}(\boldsymbol{\eta}^{(t)},\boldsymbol{\xi})\,V_j + \mathbf{b}_i^{(t)} \tag{6}$$

in which $\ddot{\mathbf{u}}_i^{(t)}$ is the second derivative of displacement of particle i at time t, $\mathbf{f}(\boldsymbol{\eta}^{(t)},\ \boldsymbol{\xi})$ denotes the pairwise bond force, N_{R_i} is the number of particles within the horizon of particle i, V_j is the volume of node j, and $\mathbf{b}_i^{(t)}$ is the body force of particle i at time t.

$$\mathbf{f}_v = \sum_{j=1}^{N_{R_i}}\mathbf{f}(t)V_j \tag{7}$$